Supporting Information

Ni_2P promotion for the high hydrogenation activity of naphthalene on wrinkle silica nanoparticles with tunable hierarchical pores sizes in a large range

Di Hu[a], Aijun Duan*[,a], Chunming Xu*[,a], Peng Zheng[a], Yuyang Li[a], Chengkun Xiao[a], Cong Liu[a], Qian, Meng[a], Huiping Li[a]

[a] State Key Laboratory of Heavy Oil Processing, China University of Petroleum-Beijing, Beijing, 102249, P. R. China.
* E-mail: duanaijun@cup.edu.cn   Tel: +86 10 89732290.

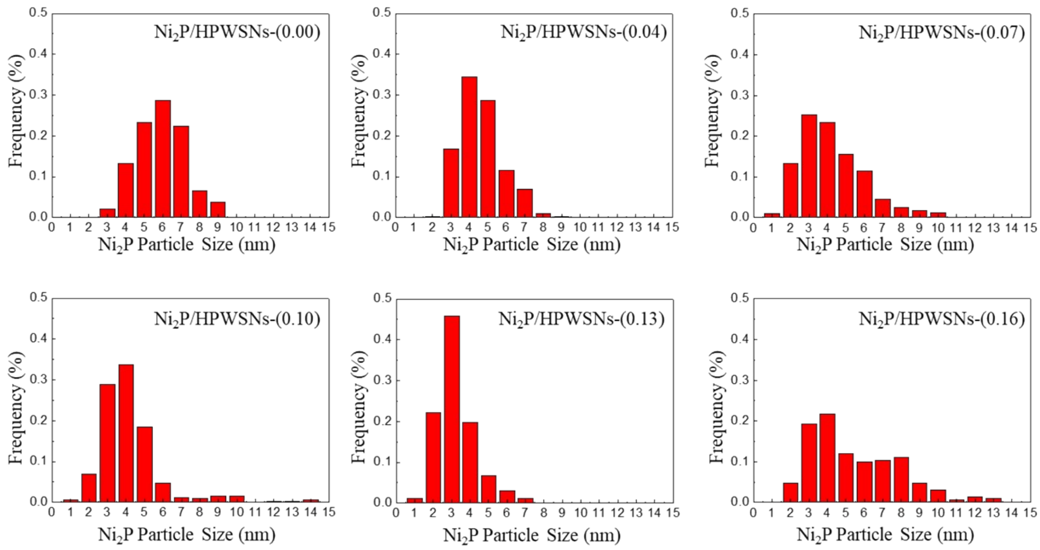

Figure S1. The size distributions of Ni_2P/HPWSNs fresh catalysts

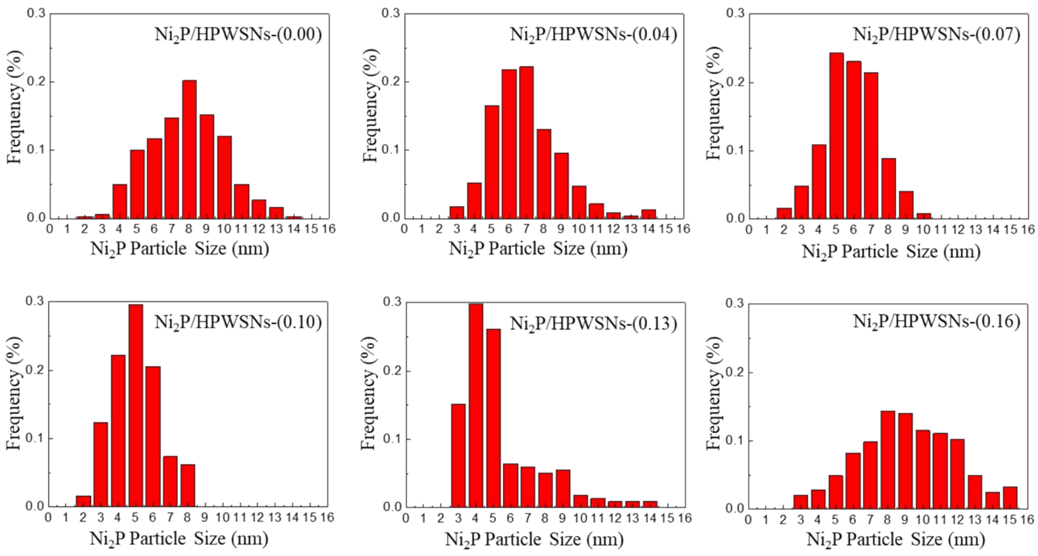

Figure S2. The size distributions of Ni_2P/HPWSNs spent catalysts after reaction

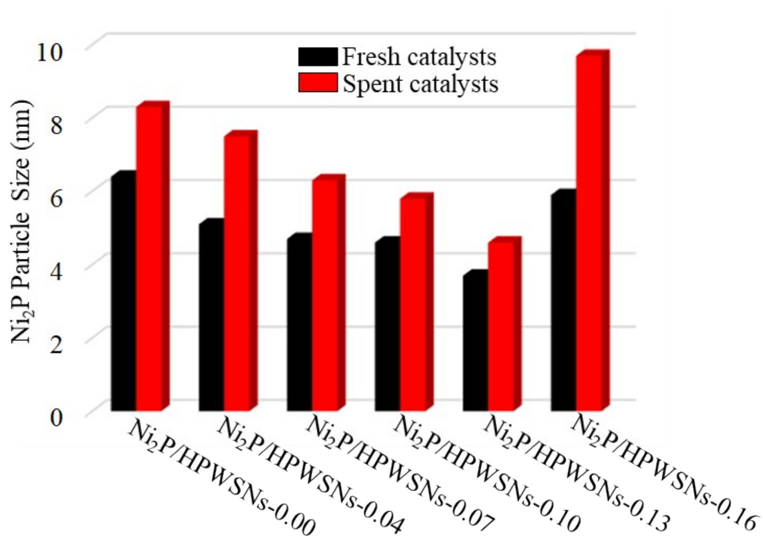

Figure S3. The size change profiles of Ni_2P particles over Ni_2P/HPWSNs series catalysts before and after reaction

It can be seen from the Figure S3 that the sizes of Ni_2P nanoparticles increased by 24.3 %~64.4% after high temperature compared to the Ni_2P nanoparticles over the fresh catalysts, among which the size change of Ni_2P particles over Ni_2P/HPWSNs-0.13 catalyst is minimum.

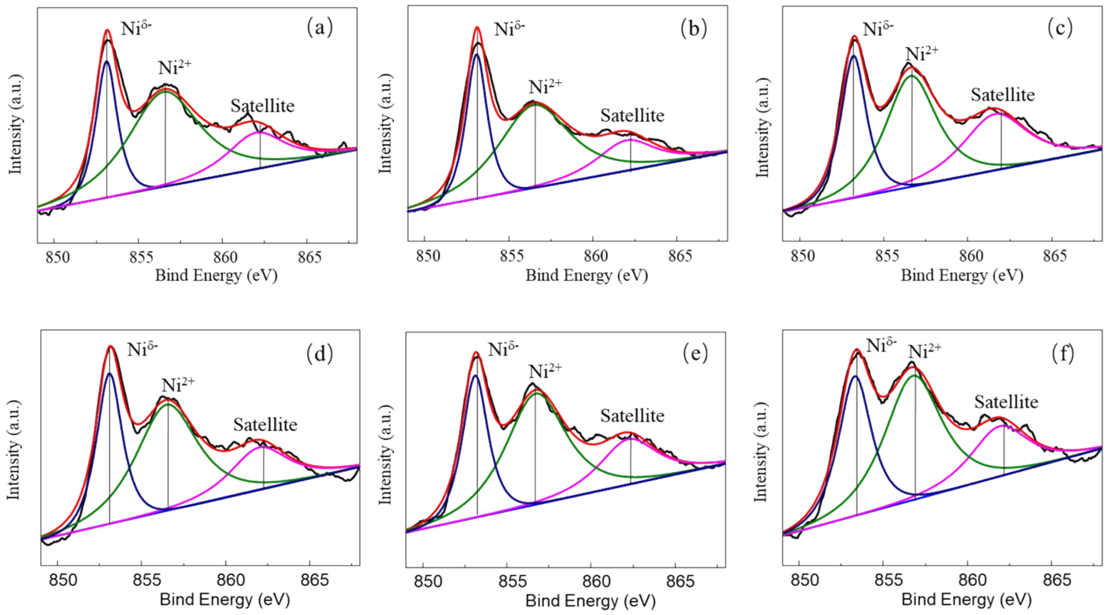

Figure S4. The XPS spectra of Ni2p in the Ni_2P/HPWSNs samples

(a) Ni_2P/HPWSNs-0.00, (b) Ni_2P/HPWSNs-0.04, (c) Ni_2P/HPWSNs-0.07

(d) Ni_2P/HPWSNs-0.10, (e) Ni_2P/HPWSNs-0.13, (f) Ni_2P/HPWSNs-0.16

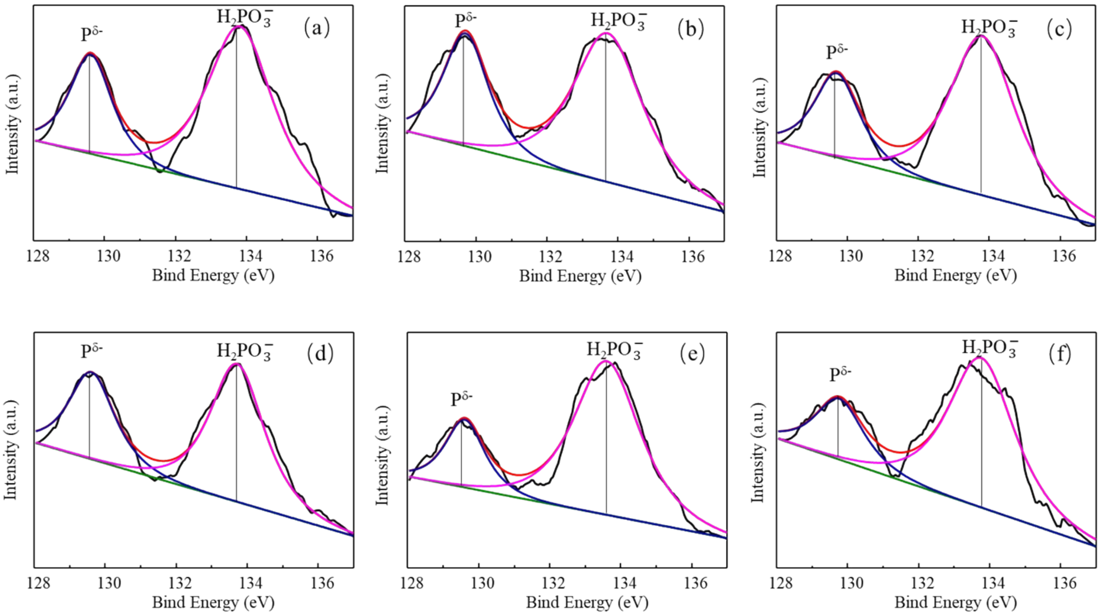

Figure S5. The XPS spectra of P2p in the Ni_2P/HPWSNs samples

(a) Ni_2P/HPWSNs-0.00, (b) Ni_2P/HPWSNs-0.04, (c) Ni_2P/HPWSNs-0.07

(d) Ni_2P/HPWSNs-0.10, (e) Ni_2P/HPWSNs-0.13, (f) Ni_2P/HPWSNs-0.16

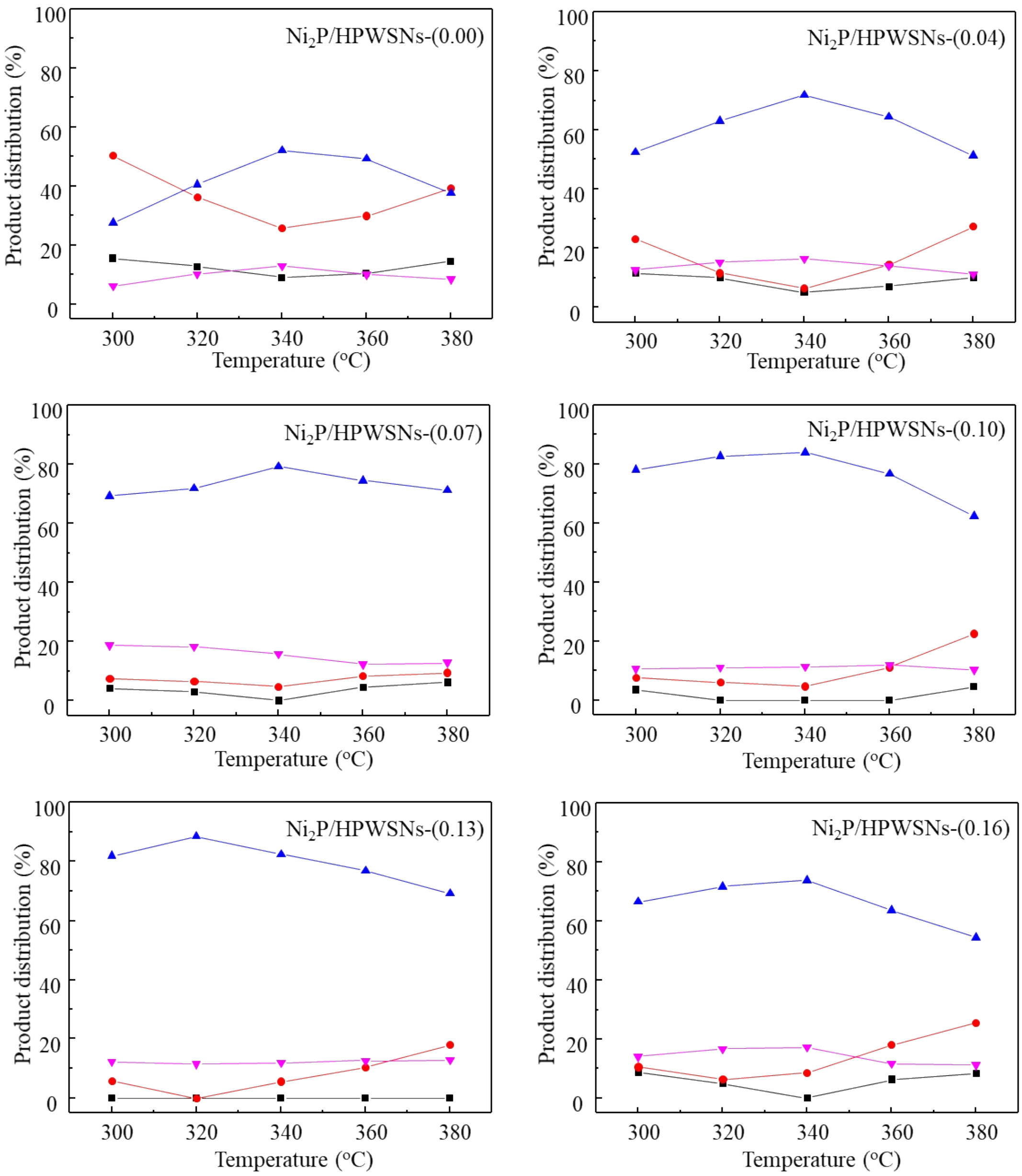

Figure S6. The product distributions on Ni$_2$P/HPWSNs series catalysts

Naphthalene **Tetralin** **Trans-decalin** **Cis-decalin**

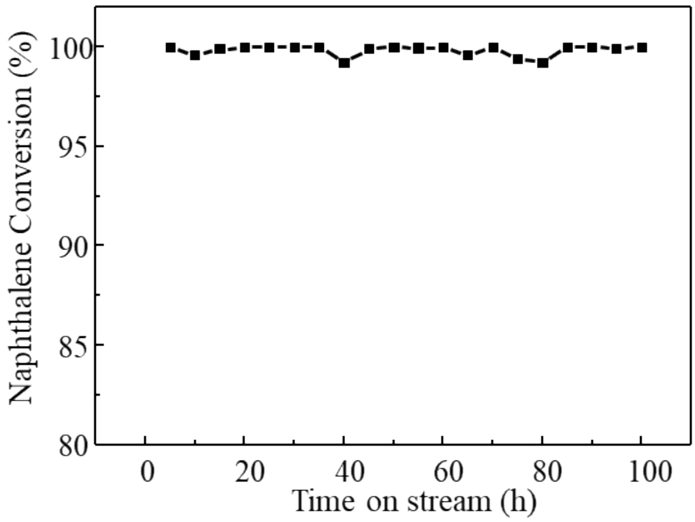

Figure S7. The hydrogenation results of naphthalene with time on stream over Ni_2P/HPWSNs-0.13 catalyst (340 ^oC, 4 MPa, 500 mL/mL and 10 h^{-1}).

The long-period (100 h) naphthalene hydrogenation experiments were complemented over Ni_2P/HPWSNs-0.13 catalyst (@340 ^oC, 4 MPa, 500 mL/mL and 10 h^{-1}). It can be seen from Figure S7 that the naphthalene conversions keep stable at around 99%~100% in the range of 0~100 h reaction on stream, indicating that the Ni_2P/HPWSNs-0.13 catalyst possesses outstanding catalytic stabilities.

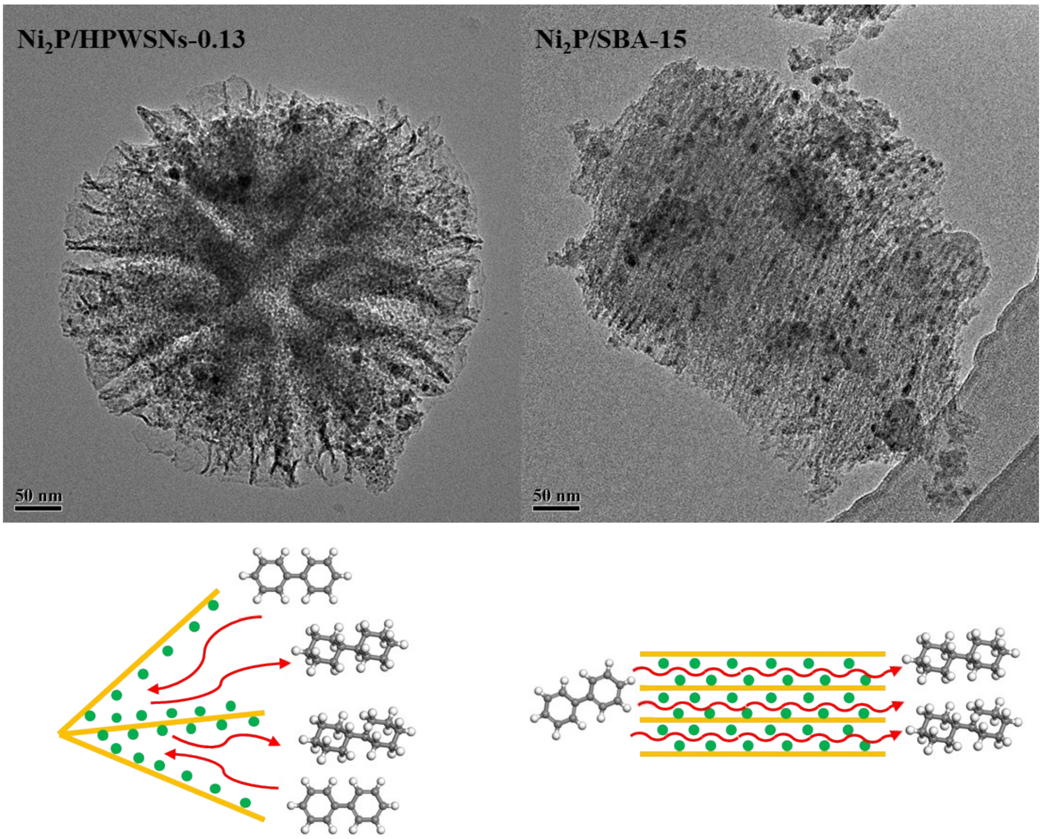

Figure S8. TEM patterns and structure schemes of Ni_2P/HPWSNs-0.13 and Ni_2P/SBA-15 catalysts

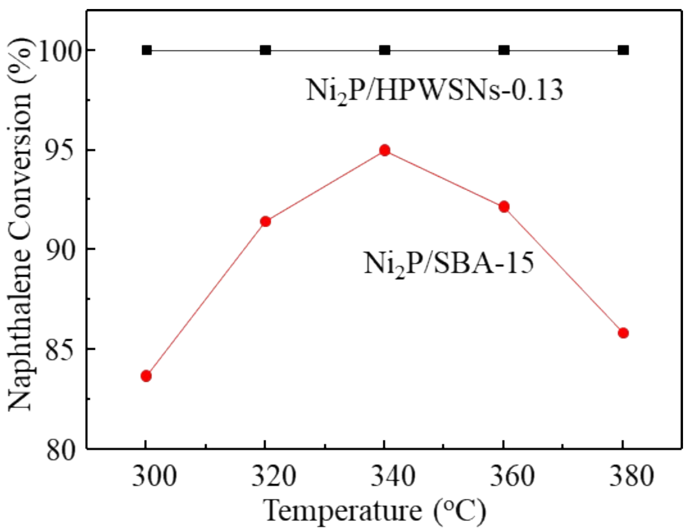

Figure S9. The naphthalene conversions of Ni_2P/HPWSNs-0.13 and Ni_2P/SBA-15 catalysts

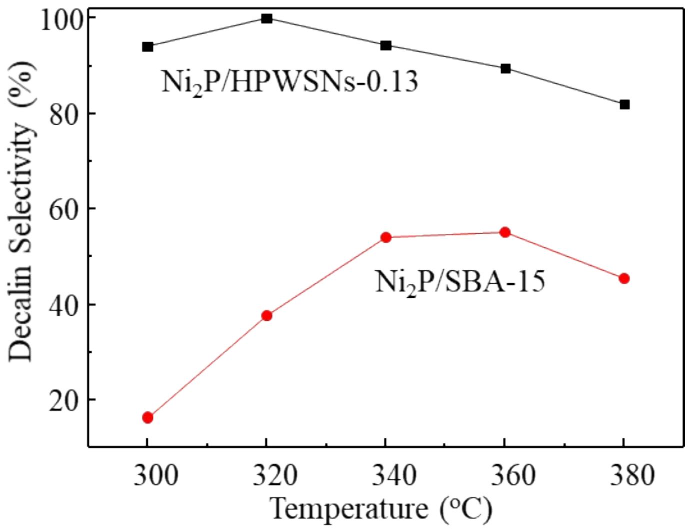

Figure S10. The decalin conversions of Ni_2P/HPWSNs-0.13 and Ni_2P/SBA-15 catalysts

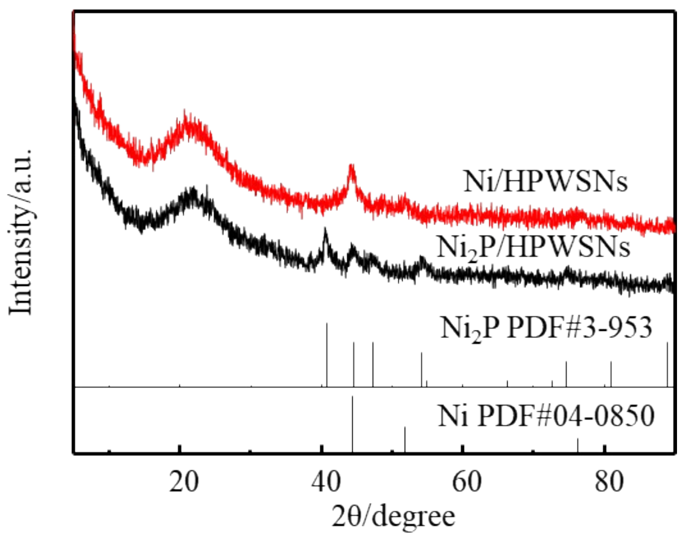

Figure S11. The comparison of XRD patterns for Ni_2P/HPWSNs and Ni/HPWSNs catalysts.

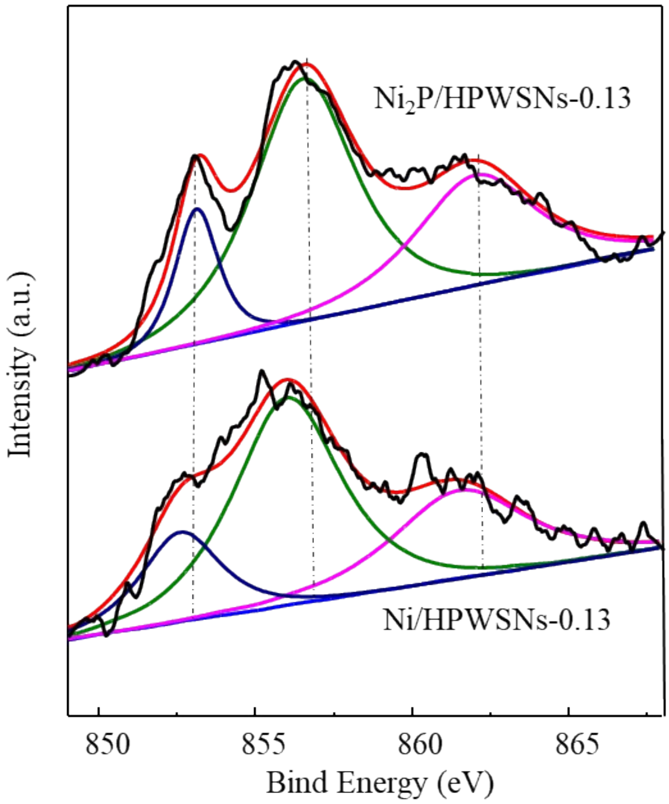

Figure S12. The comparison of XPS patterns for Ni_2P/HPWSNs and Ni/HPWSNs catalysts.

It can be seen from the XRD pattern in Figure S11 that the Ni nanoparticles of Ni/HPWSNs catalysts are reduced to metallic nickel crystallites under the same reduction conditions, while the characteristic peaks of Ni appearing 44.3^{o}, 51.8^{o} and 76.3^{o} are not found over Ni_2P/HPWSNs catalysts, confirming that no metallic nickel crystallites exist on the supported nickel phosphides catalysts after reduction. Moreover, the XPS results show that the Ni 2p signals of Ni/HPWSNs catalysts appear at lower binding energy compared to that of Ni_2P/HPWSNs catalysts, further prove the high stability of Ni_2P under the reduction condition.

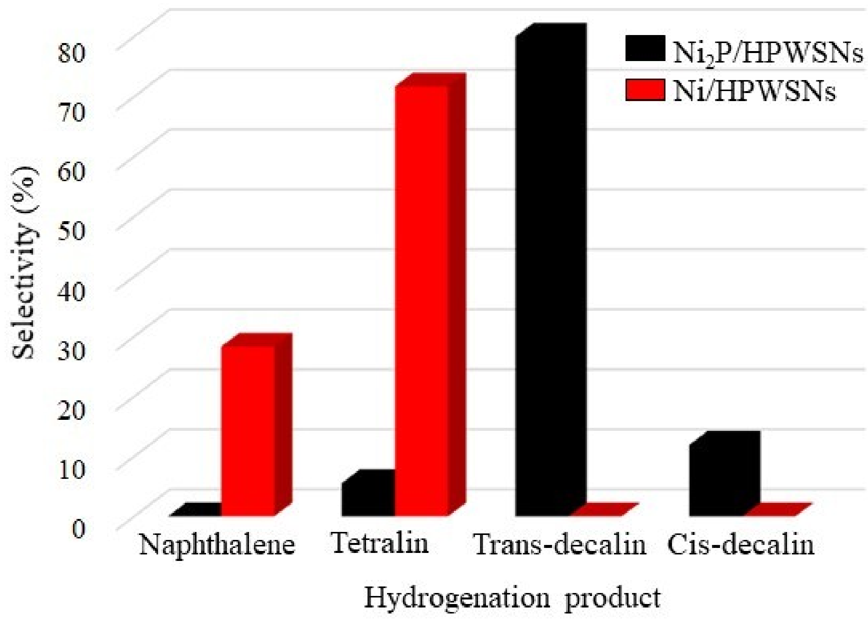

Figure S13. The comparison of product distributions for Ni_2P/HPWSNs and Ni/HPWSNs catalysts.

The differences in the hydrogenation product distributions at 340 ^{o}C over Ni_2P/HPWSNs and Ni/HPWSNs catalysts are displayed in Figure S13. The results show that the products of both trans-decalin and cis-decalin are not detected on the single Ni supported catalysts, demonstrating that it is extremely difficult for naphthalene to deeply hydrogenate into decalin over Ni/HPWSNs catalyst.